

# Highly Purified Biocompatible Gold Nanorods for Contrasted Optoacoustic Imaging of Small Animal Models

Anton V. Liopo<sup>1,\*</sup>, André Conjusteau<sup>1</sup>, Olga V. Chumakova<sup>2</sup>, Sergey A. Ermilov<sup>1</sup>, Richard Su<sup>1</sup>, and Alexander A. Oraevsky<sup>1</sup>

<sup>1</sup>TomoWave Laboratories, Houston, TX 77081, USA

<sup>2</sup>Department of Integrative Biology and Pharmacology, University of Texas Health Science Center Houston, TX 77030, USA

We developed a methodology for high yield synthesis of gold nanorods (GNR) with narrow band optical absorption centered at 760 nm. GNR were purified from hexadecyltrimethylammonium bromide (CTAB) and coated with polyethylene glycol (PEG). The molar ratio between GNR and PEG (1 ÷ 50000) was optimized to make the conjugate a biocompatible PEG-GNR contrast agent for optoacoustic (OA) imaging. *In vitro* toxicity studies showed no significant change in survival rates of cultured normal (IEC-6, MDCK) and cancer (SKBR3 and HEPG2) cells after they were incubated with 0.125 to 1.25 nM PEG-GNR solutions. *In vivo* toxicity studies in nude mice showed no pathological changes in liver after the IV injection of GNR. Significant enhancements of OA contrast in comparison to images of untreated mice were observed 1 hour after the GNR injection in a dose of 20 mg gold per kg of body mass.

**Keywords:** Pegylated Gold Nanorods, Optoacoustic Tomography of Mice, Cell Particle Interactions.

## 1. INTRODUCTION

Gold nanoparticles of various shapes have been proposed as contrast agents for biomedical imaging, thermal therapy, and chemical sensing.<sup>1,2</sup> One type of gold nanoparticles with a strong tunable plasmon resonance in the near-infrared spectral range is GNR.<sup>3,4</sup> After intravenous administration, GNR get distributed inside the body. Increase of local concentration of GNR within endothelium vascular cells, or inside organs, will result in the enhancement of optical and optoacoustic contrast due to the intense Plasmon resonance of GNR.<sup>5,6</sup> GNR stabilized with CTAB showed strong cytotoxicity.<sup>7</sup> For *in vivo* applications, PEG modification of GNR is usually performed by adding PEG-SH to the CTAB solution, followed by the removal of the excess CTAB via dialysis or centrifugation.<sup>6-8</sup> The reasons for PEGylation (i.e., the covalent attachment through thiol terminated PEG<sup>9</sup>) of nanoparticle surfaces include shielding of antigenic and immunogenic epitopes, shielding receptor-mediated uptake

by the reticuloendothelial system (RES), and preventing recognition and degradation by proteolytic enzymes.<sup>10</sup> PEG-modified GNR showed a negative surface potential,<sup>4</sup> as well as low level cytotoxicity *in vitro*,<sup>7</sup> and can therefore be used for biomedical applications such as OA imaging.<sup>5</sup> Three-dimensional OA tomography was successfully used to visualize the blood circulation system and certain blood-rich organs, like kidneys and spleen, within live mice with and without nanoparticle contrast agents.<sup>11,12</sup> Methods for enhancing the contrast of OA images with strongly absorbing gold nanoparticles were previously discussed.<sup>1,13</sup> In these studies, we adopted the published methodology of GNR fabrication<sup>14,15</sup> to produce a high yield of GNR with narrow band optical absorption centered at 760 nm. The nanorods were PEGylated to become non-toxic in animals, and were injected intravenously in the mice's tails as biocompatible OA contrast agents. Observation of contrast enhancement of mouse imaging was performed with LOIS-3D optoacoustic tomographic system (TomoWave Laboratories Inc., Houston, TX USA).

Our report is focused on three GNR-related aspects: First, the stability of GNR-PEG conjugates upon removal of CTAB. Second, the toxicity of PEG-GNR conjugates

\*Author to whom correspondence should be addressed.

in several cell lines as well as *in vivo*. Third, OA contrast enhancement following IV administration of PEG-GNR.

## 2. MATERIALS AND METHODS

### 2.1. Fabrication, PEGylation of GNR, and Their Characterization

We previously described a general strategy for the synthesis and stabilization of GNR with thiol-terminal polyethylene glycol (mPEG-thiol or PEG in this report) which displaces the original bilayer of surfactant CTAB to provide biocompatibility of the resulting optoacoustic contrast agent.<sup>13,16</sup> This procedure<sup>15</sup> resulted in synthesis of GNRs with a narrow-band optical absorption around 760 nm. After the GNR solution underwent low speed centrifugation at 1000× g for 20 min, the pellet was discarded and the supernatant was centrifuged again at 10,000× g for 15 minutes. The supernatant was then discarded and the pellet resuspended in deionized water for PEGylation. We slightly modified the PEGylation method previously reported:<sup>7</sup> for this 1.0 mL of 2 mM potassium carbonate was added to 8 mL of aqueous 625 pM GNR solution and 1.0 mL of mPEG-Thiol-5000 (molecular weight 5000, Laysan Bio Inc.) in concentration from 0.05 to 0.5 mM for optimization of PEGylation. Phosphate buffer solution (PBS) at pH 7.4 was used for the final resuspension of GNR-PEG and the conjugate was filtered through a 0.22 μm Millipore Express Plus membrane. The control for spectral properties of GNR (UV-VIS spectra into range 400–1100 nm) was by Beckman 530 and Thermo Scientific Evolution 201 Spectrophotometer). The zeta-potential of GNR before and after conjugation was measured with a high performance Zetasizer (Malvern Instruments Ltd., Southborough, MA, USA) at 25 °C, and ten 20-second runs were performed for each sample.

### 2.2. Cell Culture, Viability and Cell Proliferation

Cell lines SKBR3 (Human breast adenocarcinoma), HEPG2 (Human liver hepatocellular epithelium carcinoma), IEC-6 (Rat small intestine normal epithelial cells) and MDCK (Dog kidney normal epithelial cells) were obtained from American Type Culture Collection (ATCC) and were cultured in essential media with 10% fetal bovine serum.

Cell viability was determined using a kit for the detection of LDH (Roche). Cell survival following PEG-GNR incubation in different concentrations (125–250 pM) and with various ratios between number of molecules of PEG and GNR (10000–100000) was monitored. SKBR-3 cells were seeded into a 96-well plate at a density of  $2 \times 10^5$  cells/ml in 0.1 ml of media per well. 25 μl samples of the media were then collected (after 24 h incubation with PEG-GNR) at indicated arch independence points in the LDH assay kit. The experimental condition was

measured using the maximum amount of releasable LDH enzyme activity, which is determined by lysing the cells with 1% Triton X-100 in medium (at this concentration, Triton X-100 does not affect the LDH activity). Cytotoxicity was calculated as the ratio between LDH release from cells to medium ( $LDH_R$ ) to total level of LDH ( $LDH_C$  from cells after Triton application plus  $LDH_R$ ) for each experimental condition of PEG-GNR incubation.

Cell proliferation was determined by examining the conversion of MTT to a purple formazan product by metabolically active cells using a kit (Roche). SKBR-3 cells were used in the same plate (after removing the medium for  $LDH_R$  assay) and the MTT assay was performed on the pretreated PEG-GNR cells. Absorbance of the LDH and MTT products was measured on a plate spectrophotometer (Bio-Tek Instruments, Inc.). Data for  $LDH_R$ , MTT conversion and  $LDH_R$ /MTT ratios, were measured and calculated from 3–4 replicates. The second technique to assess cell viability is based on trypan blue (Sigma) dye exclusion.<sup>17</sup> The cells were incubated 5 min with 0.4% trypan blue, and counted as a percentage of stained cells to total number of cells. This staining was used for investigation of cell viability depending on concentrations of GNR-PEG (from 125 to 1250 pM) after 24 hours incubation with IEC-6, MDCK and HEPG2 cells as well as for measuring surviving these cells their after incubation with GNR-PEG and GNR-CTAB (both at 500 pM) after 48 hours. As positive control, we used cells to which only PBS solution (pH 7.4) was added. Correspondingly, knowingly toxic CTAB-coated GNR solutions<sup>7</sup> were added in the same concentrations as pegylated GNR, and these samples were used as negative controls in each experimental condition.

### 2.3. Histology

Selected mice were sacrificed at 72 and 192 h after the IV injections of GNRs. Liver extractions were produced as paraffin-embedded slices for SS and HE staining. Tissue sections (5 μm) were deparaffinized and rehydrated through xylene (3 changes, 5 min each) and graded ethanol solutions from 100 to 50% (1 min each). After this, samples were rinsed in dH<sub>2</sub>O and placed in a water bath for 10 min with tris-buffered saline with Tween 20 (TBST, Dako, Denmark). Retrieval with Target Retrieval Solution pH 6.1 (TRS, Dako, Denmark) was then performed in a preheated container at 96–99 °C for 30–40 min. The slides of liver sections were stained for PEG-GNR optical visualization with a SS Kit (BBI International, UK) according to manufacturer instruction, and HE stained for analysis of possible pathological consequences in liver after PEG-GNR administration.

### 2.4. Optoacoustic Imaging System

A commercial prototype of a three-dimensional optoacoustic tomography system developed for preclinical research

at TomoWave Laboratories (USA) was used in this study.<sup>11,12</sup> The OA mouse imaging system consists of four main components: fiber-optic light delivery, mouse holder with translation and rotation, detector array of 64 transducers, and data acquisition and imaging electronics. Optical illumination was obtained from a pulsed Ti:Saph laser (Quanta Systems, Italy) tuned at 765 nm with a 10 Hz repetition rate and an energy of  $\sim 70$  mJ per 12 ns pulse. Heating elements and PID temperature controller ensured the water temperature was maintained at  $36 \pm 0.1$  °C. The mouse holder with gas anesthesia delivery module (Summit Anesthesia Solutions) was described in detail in our previous work.<sup>11</sup> The collected optoacoustic signals were amplified, digitized, and acquired at each rotational position of the mouse.<sup>11,12</sup>

We used Athymic Nude-Foxn1<sup>nu</sup> mice (Harlan), 7–9 weeks old, weighing about 25 g. Animal handling, isoflurane anesthesia, and euthanasia were described in detail in our publications<sup>11,12</sup> and mouse-related procedures were in compliance with our Institutional Animal Care and Use Committee (IACUC) protocol. Each mouse was scanned prior to injection of GNR solution to provide the control OA images. After the initial scan, the mouse was taken out of the water tank and had 400  $\mu$ l of GNR in sterile PBS injected intravenously (IV) through the tail vein. The injected solution contained  $7.5 \times 10^{12}$  GNR/ml or 12.5 nM, which is equivalent to 150–250 pM after distribution within the mouse's body. The optoacoustic scans were repeated 1 hour following the GNR injection to monitor the evolution of optoacoustic contrast.

### 3. RESULTS

Purification of GNR through centrifugation and filtration was performed to increase the uniformity of the GNR fraction. The results of centrifugation (needed to discard unwanted pellets) can be seen in Figure 1. Furthermore, filtration caused negligible alteration of the GNR pectral

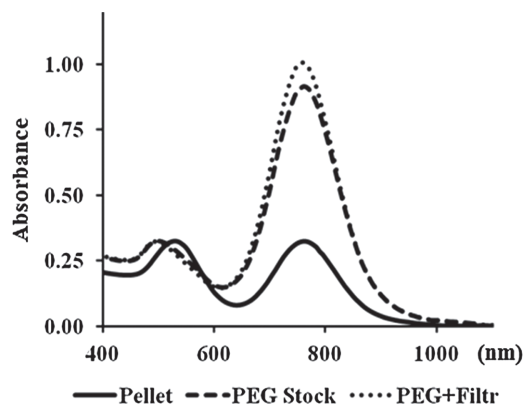


**Fig. 1.** Absorption spectra of GNR: after low speed centrifugation of GNR-CTAB (Pellet), after PEGylation of GNR (PEG Stock), and after filtration of GNR-PEG (PEG-Filtr). Spectra are normalized to match the short wavelength peak of the PEG Stock data.

properties. These purification steps at the end of GNR production resulted in a narrow peak around 760 nm.

We investigated the influence of concentrations of GNR-PEG conjugates on the physiological status of cell cultures at different ratios between GNR and PEG. In this set of experiments, two types of cells (SKBR3 and MDCK) were incubated with GNR-PEG (Tables I and II).

For the sake of brevity, only data for SKBR3 cells are reported here as our data for MDCK line showed similar trends. The effect of GNR-PEG was estimated using MTT level, activity of LDH<sub>R</sub>, and LDH<sub>C</sub> (Table I). We also calculated the ratios of LDH<sub>R</sub> to total LDH (LDH<sub>R</sub> + LDH<sub>C</sub>) and LDH<sub>R</sub>/MTT after 24 h treatment with GNR-PEG (molar ratios were 10000, 20000, 50000 and 100000).

We observed only minor differences in all parameters for GNR-PEG conjugates with ratios more than 50000. Low molar ratio, such as 20000 or 10000, resulted in toxic effects suppressing cell proliferation (MTT and their ratio with LDH) and damaging cells membranes. From these experiments we can conclude that the optimum molar ratio between GNR and PEG is near 50000.

To confirm the chemistry modification and stability of GNR-PEG conjugates we investigated the Zeta-potential. It was measured for GNR-CTAB, GNR-PEG and thoroughly washed GNR-PEG after 3 h incubation in 5% bovine serum albumin (BSA, pH 7.4) solution. The GNR-CTAB nanoparticles have a positive charge after synthesis. After PEGylation, a negative zeta-potential confirmed chemistry changes to the GNR surface: the CTAB bi-layer was removed (Table III). Stability of GNR-PEG conjugates was observed as the surface charge did not change in a statistically significant manner after incubation in isotonic 5% Bovine Serum Albumin (BSA) in PBS with 5% Glucose at pH 7.4, which simulates blood plasma osmolarity. This therefore indicates BSA does not modify the surface of pegylated GNR, confirming stability.

Figure 2 shows how cell viability depends upon concentration of GNR-PEG for a molar ratio of 1:50000 (0.5 nM GNR-CTAB mixed with 25  $\mu$ M of PEG). After incubation with different concentration of GNR-PEG, cells stained with trypan blue were counted as a percentage of the total amount of IEC-6, MDCK and HEPG2 cells (Fig. 2(A)). Figure 2(B) shows results for the same types of cells but after incubation with GNR-PEG or GNR-CTAB conjugates, both in concentration of 0.5 nM ( $n = 5$ ). GNR-PEG did not show damaging effects on cells in low concentrations (1.0 nM and below) with non-significant trend for a concentration of 2 nM. Significantly increased cell death, in comparison to control, was apparent only for GNR-PEG at a concentration of 5 nM, as well as GNR-CTAB incubation at 0.5 nM.

Slices of excised liver tissue shown in Figure 3 were taken from another set of mice to track the accumulation of GNR as well as possible toxicity effects over a span of eight days. Silver staining images demonstrate a visible

**Table I.** Cell proliferation (MTT assay), LDH release ( $LDH_R$ ) into medium, and total quantity of LDH in SKBR3 cells after their membrane are destroyed with Triton X100 ( $LDH_C$ ). 24 hours incubation with different GNR-PEG of different compositions (different molar ratio of PEG to GNR) 3 independent measurements,  $M \pm SD$ .

		Concentration of GNR conjugates in cell medium (nM)				
SKBR3		Control	0.125	0.250	0.500	1.250
<b>MTT</b>						
	<b>CTAB</b>	$0.81 \pm 0.024$	$0.79 \pm 0.008$	$0.74 \pm 0.081$	$0.48 \pm 0.112^b$	—
	<b>10000</b>	$0.81 \pm 0.024$	$0.74 \pm 0.018$	$0.71 \pm 0.070$	$0.61 \pm 0.012^a$	$0.50 \pm 0.012^b$
	<b>20000</b>	$0.81 \pm 0.024$	$0.75 \pm 0.018$	$0.73 \pm 0.019$	$0.63 \pm 0.017^a$	$0.59 \pm 0.036^b$
	<b>50000</b>	$0.81 \pm 0.024$	$0.81 \pm 0.032$	$0.84 \pm 0.030$	$0.73 \pm 0.073$	$0.64 \pm 0.065^a$
	<b>100000</b>	$0.81 \pm 0.024$	$0.94 \pm 0.020$	$0.86 \pm 0.067$	$0.74 \pm 0.059$	$0.69 \pm 0.095$
<b>LDH, release from cells into medium (<math>LDH_R</math>)</b>						
Molar ratio	<b>CTAB</b>	$0.11 \pm 0.019$	$0.10 \pm 0.035$	$0.22 \pm 0.076^a$	$0.62 \pm 0.278^b$	—
	<b>10000</b>	$0.11 \pm 0.019$	$0.09 \pm 0.013$	$0.11 \pm 0.014$	$0.11 \pm 0.038$	$0.25 \pm 0.057^a$
PEG and GNR (numbers)	<b>20000</b>	$0.11 \pm 0.019$	$0.11 \pm 0.013$	$0.08 \pm 0.009$	$0.09 \pm 0.005$	$0.20 \pm 0.047^a$
	<b>50000</b>	$0.11 \pm 0.019$	$0.09 \pm 0.026$	$0.07 \pm 0.026$	$0.10 \pm 0.017$	$0.15 \pm 0.050$
	<b>100000</b>	$0.11 \pm 0.019$	$0.10 \pm 0.059$	$0.09 \pm 0.034$	$0.11 \pm 0.031$	$0.15 \pm 0.035$
<b>LDH after destruction of the cell membranes (<math>LDH_C</math>)</b>						
	<b>CTAB</b>	$1.35 \pm 0.077$	$1.23 \pm 0.024$	$1.08 \pm 0.068^a$	$0.55 \pm 0.240^b$	—
	<b>10000</b>	$1.35 \pm 0.077$	$1.25 \pm 0.051$	$1.18 \pm 0.079$	$1.21 \pm 0.076^a$	$0.82 \pm 0.157^b$
	<b>20000</b>	$1.35 \pm 0.077$	$1.21 \pm 0.021$	$1.15 \pm 0.027$	$1.20 \pm 0.044^a$	$1.12 \pm 0.105^b$
	<b>50000</b>	$1.35 \pm 0.077$	$1.31 \pm 0.052$	$1.23 \pm 0.097$	$1.20 \pm 0.166$	$1.15 \pm 0.175$
	<b>100000</b>	$1.35 \pm 0.077$	$1.31 \pm 0.011$	$1.28 \pm 0.037$	$1.31 \pm 0.021$	$1.18 \pm 0.123$

<sup>a</sup> $P < 0.05$ ; <sup>b</sup> $P < 0.01$  as compared with control, symbol (—) indicates complete death of the cells.

**Table II.** Normalization of the LDH release through total LDH ( $LDH_C + LDH_R$ ) and MTT, all abbreviations are the same as in Table I.

		Concentration of GNR conjugates in cell medium (nM)				
SKBR3		Control	0.125	0.250	0.500	1.250
<b><math>LDH_R / (LDH_C + LDH_R)</math></b>						
	<b>CTAB</b>	$0.07 \pm 0.013$	$0.07 \pm 0.025$	$0.17 \pm 0.044^a$	$0.53 \pm 0.034^b$	—
	<b>10000</b>	$0.07 \pm 0.013$	$0.06 \pm 0.008$	$0.09 \pm 0.013$	$0.08 \pm 0.034$	$0.23 \pm 0.036^b$
	<b>20000</b>	$0.07 \pm 0.013$	$0.08 \pm 0.009$	$0.06 \pm 0.008$	$0.08 \pm 0.005$	$0.15 \pm 0.042^a$
	<b>50000</b>	$0.07 \pm 0.013$	$0.07 \pm 0.017$	$0.05 \pm 0.023$	$0.08 \pm 0.012$	$0.12 \pm 0.029$
	<b>100000</b>	$0.07 \pm 0.013$	$0.07 \pm 0.039$	$0.07 \pm 0.024$	$0.08 \pm 0.021$	$0.12 \pm 0.031$
<b><math>LDH_R / MTT</math></b>						
	<b>CTAB</b>	$0.13 \pm 0.025$	$0.12 \pm 0.045$	$0.30 \pm 0.070^a$	$1.26 \pm 0.360^b$	—
	<b>10000</b>	$0.13 \pm 0.025$	$0.11 \pm 0.015$	$0.16 \pm 0.020$	$0.18 \pm 0.067$	$0.50 \pm 0.125^b$
	<b>20000</b>	$0.13 \pm 0.025$	$0.14 \pm 0.020$	$0.11 \pm 0.014$	$0.15 \pm 0.003$	$0.33 \pm 0.114^a$
	<b>50000</b>	$0.13 \pm 0.025$	$0.11 \pm 0.036$	$0.08 \pm 0.033$	$0.14 \pm 0.012$	$0.23 \pm 0.078$
	<b>100000</b>	$0.13 \pm 0.025$	$0.11 \pm 0.061$	$0.11 \pm 0.041$	$0.15 \pm 0.036$	$0.20 \pm 0.056$

increase of GNR within the liver from day one up to three days following the injection. However, after eight days, it seems that amount of GNR decreases. The studies with hematoxylin and eosin (HE) staining showed no visible differences between the PBS control and the GNR slices.

**Table III.** Zeta-Potential (mV) for CTAB coated GNR before PEGylation (GNR-CTAB), GNR after PEGylation (GNR-PEG) and PEGylated GNR after incubation with 5% BSA in PBS, pH 7.4, 3 hours (GNR-PEG+BSA) (mean  $\pm$  SD,  $n = 8$ ).

GNR Modification	Nanoparticle ZP (mV)
<b>GNR-CTAB</b>	$50.7 \pm 18.12$
<b>GNR-PEG</b>	$-19.9 \pm 10.01$
<b>GNR-PEG in BSA</b>	$-13.7 \pm 10.58$

From the HE staining we cannot confirm any morphological changes in mice liver caused by the GNR.

OA images are shown for pre-GNR injection, and one hour after PEG-GNR injection in Figure 4. We can clearly see an increase in number of distinguishable bright objects (blood vessels and organs) an hour following the GNR injection. Peripheral blood vessels around the back, ribs, and underneath the arms are most enhanced. Vertebrae, interestingly enough, are also quite apparent during this time, with various vertebrae discs of the mouse being visualized.

## 4. DISCUSSION

GNR exhibit localized surface plasmon resonance (LSPR) which is manifested by an absorption band in the visible

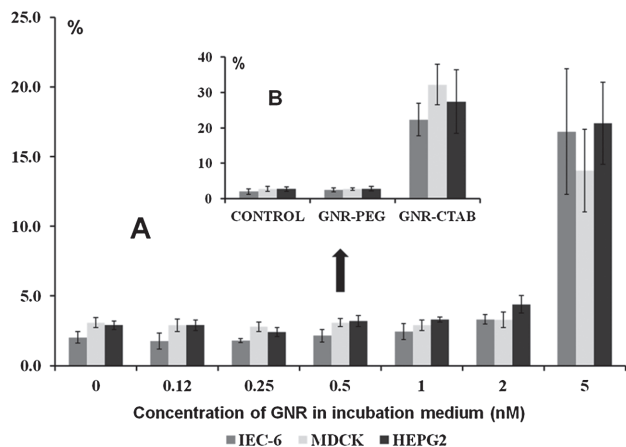


**Fig. 2.** Dose dependence effects of GNR on IEC-6, MDCK and HEPG2 cell lines: (A) Percentage of dead cells after staining with Trypan Blue and (B) Percentage of dead cells after incubation with GNR coated with CTAB or PEG.

or near infrared (NIR) region of the optical spectrum.<sup>2,3</sup> Purification steps presented in this study resulted in a narrow absorption peak around 760 nm that matches the biological transparency window.<sup>18,19</sup> GNR are grown from colloidal gold seeds in the presence of a surfactant: CTAB.<sup>14,15</sup> If CTAB is removed from the solution, the nanorods immediately aggregate.<sup>20</sup> Several strategies have been developed to modify the surface chemistry of nanorods, including polyelectrolyte wrapping to bind the CTAB layer, displacement by alkanethiols or lipids, displacement of the CTAB layer by a thiol-terminal PEG.<sup>4,7,20</sup> It was determined that 5000 MW PEG-SH ligand has a “footprint” around 0.35 nm,<sup>2,21</sup> somewhat larger than the CTAB – 0.22 nm.<sup>2,4</sup> CTAB binding is believed to take place via a gold-bromide surfactant complex. The bromide ion is thought to be the bridge between the gold surface and the positively charged quaternary nitrogen atom of the surfactant,<sup>14</sup> thus generating van der Waals coupling with the gold surface. Because the

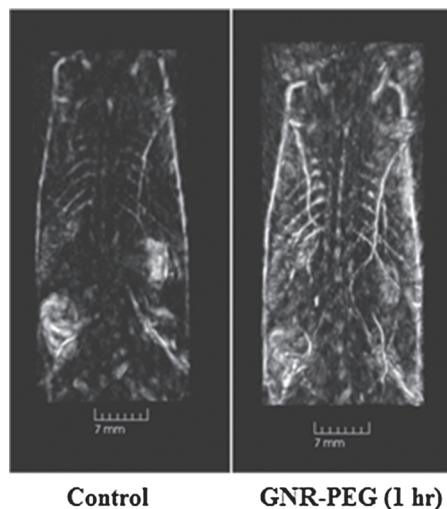


**Fig. 4.** Optoacoustic images of nude mice before, and 1 hour after, intravenous injection of PEG-GNR ( $3 \times 10^{12}$  GNR per mouse).

Delivered by Ingenta to:

gold-thiol bond is covalent in nature,<sup>9</sup> it is stronger than CTAB's bond being the combination of weak van der Waals and electrostatic interactions.

The adopted fabrication procedure yields GNR with dimensions of 50 by 15 nm: the total surface area is therefore around 2800 nm<sup>2</sup>. Consequently, each GNR could be surrounded by 13000 CTAB molecules at maximum packing density, and by 8000 molecules of PEG after complete PEGylation. However, after PEGylation a number of CTAB molecules can stay on surface of GNR and slowly detach in the cell or *in vivo*. The resulting CTAB concentration will be insignificant: GNR-PEG conjugates have not shown toxic effects.<sup>4</sup> Our GNR-PEG complexes were stable for several months, consistent with the data reported by other groups.<sup>6,7,20</sup>

Biological optimization of PEGylation was investigated through cell viability and proliferation using different cell lines. We used two techniques to assess cell viability, and cell proliferation was determined by MTT assay. Combined data on LDH release, MTT conversion, and LDH<sub>R</sub>/MTT ratios (Tables I, II, and Fig. 2) were necessary for biooptimization of the GNR PEGylation protocol. The percentage of dead cells assessed with Trypan blue demonstrated absence of toxicity for PEGylated GNR in a big range of concentrations up to 2.0 nM (IEC-6 cells) after 24 hours of incubation and up to 0.5 nM or  $3 \times 10^{11}$  GNR/ml (SKBR-3, MDCK and IEC-6 cells) after 48 hours of incubation. This concentration is consistent with reported levels of GNR-PEG in blood or tissue after IV administration *in vivo*.<sup>12,22,23</sup> The change of zeta-potential from positive to negative after GNR PEGylation (Table III) confirmed the surface chemistry, i.e., that CTAB was removed. The new complex of PEG-GNR was stable, because PEG-GNR conjugates did not significantly display a change of surface charge after incubation in BSA solution PBS.<sup>4</sup>

gold-thiol bond is covalent in nature,<sup>9</sup> it is stronger than CTAB's bond being the combination of weak van der Waals and electrostatic interactions.

The adopted fabrication procedure yields GNR with dimensions of 50 by 15 nm: the total surface area is therefore around 2800 nm<sup>2</sup>. Consequently, each GNR could be surrounded by 13000 CTAB molecules at maximum packing density, and by 8000 molecules of PEG after complete PEGylation. However, after PEGylation a number of CTAB molecules can stay on surface of GNR and slowly detach in the cell or *in vivo*. The resulting CTAB concentration will be insignificant: GNR-PEG conjugates have not shown toxic effects.<sup>4</sup> Our GNR-PEG complexes were stable for several months, consistent with the data reported by other groups.<sup>6,7,20</sup>

Biological optimization of PEGylation was investigated through cell viability and proliferation using different cell lines. We used two techniques to assess cell viability, and cell proliferation was determined by MTT assay. Combined data on LDH release, MTT conversion, and LDH<sub>R</sub>/MTT ratios (Tables I, II, and Fig. 2) were necessary for biooptimization of the GNR PEGylation protocol. The percentage of dead cells assessed with Trypan blue demonstrated absence of toxicity for PEGylated GNR in a big range of concentrations up to 2.0 nM (IEC-6 cells) after 24 hours of incubation and up to 0.5 nM or  $3 \times 10^{11}$  GNR/ml (SKBR-3, MDCK and IEC-6 cells) after 48 hours of incubation. This concentration is consistent with reported levels of GNR-PEG in blood or tissue after IV administration *in vivo*.<sup>12,22,23</sup> The change of zeta-potential from positive to negative after GNR PEGylation (Table III) confirmed the surface chemistry, i.e., that CTAB was removed. The new complex of PEG-GNR was stable, because PEG-GNR conjugates did not significantly display a change of surface charge after incubation in BSA solution PBS.<sup>4</sup>

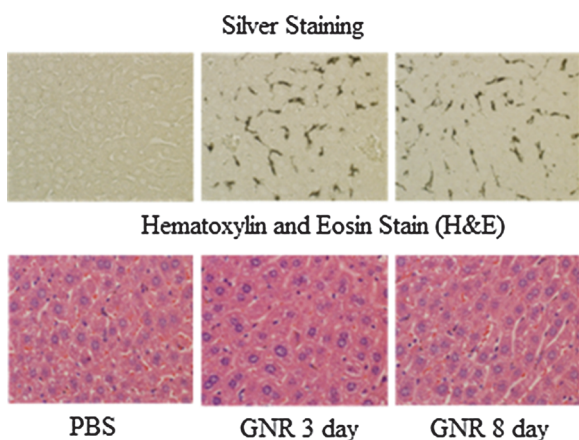


**Fig. 3.** Silver staining and Hematoxylin & Eosin stain of PEGylated GNR accumulated in mouse liver following intravenous injection.

HE staining did not show a visible difference between the PBS control and the GNR slices of liver tissue excised 8 days after IV administration of GNR-PEG conjugates (Fig. 3). The results are consistent with those reported by other groups<sup>22,23</sup> for similar dosage of GNR (around 10–20 mg/kg body mass), and are presented solely as confirmation our GNR-PEG complexes are non-toxic. We present SS data showing for the first time dynamic accumulation of PEG-GNR (Fig. 3) into liver Kupffer cells. These cells are specialized macrophages located in the liver and lining the walls of the sinusoids, and are responsible for removing non metabolized compounds from the organism. They are an important part of the reticuloendothelial system.<sup>10</sup> Our data is consistent with other reports describing no dangerous physiological changes following the administration of gold nanoparticles or nanorods *in vivo*<sup>19,22–24</sup> for small animal model of optoacoustic imaging. For OA imaging we used PEG-GNR IV in dose  $7.5 \times 10^{11}$  GNR/ml, or 20 mg/kg/BW of mouse from optimized protocol of PEGylation (Fig. 4). The OA images showed that the enhancement of brightness visible on 760 nm optoacoustic images was interpreted as local accumulation of GNRs.

## 5. CONCLUSION

In this study we demonstrated that a combination of low and high speed centrifugation of GNR before and after PEGylation provided nontoxic PEG-GNR conjugates with stable plasmon resonance. In addition, filtration of GNR furthered purification and sterilization for *in vivo* applications. We successfully optimized a protocol of GNR PEGylation to be suitable as an OA *in vivo* contrast agent. The proposed optimal PEGylation ratio was around 50000 and can be used for any molecular weight PEG. The toxicity of the fabricated and purified PEG modified GNR which were injected intravenously in the mice was determined to be minimal or none as evaluated via cell viability and proliferation standard tests. GNR distributed themselves within the circulatory system of mice within an hour and provided significant increase of optoacoustic contrast within the peripheral circulatory system. Our data showed that it is possible to track intravenously administered GNR using optoacoustic imaging without dangerous consequences for the animal.

**Acknowledgments:** This work was supported by research grants from the National Institutes of Health (R43ES021629, R44CA110137 and R44CA110137-05S1).

We are thankful Dr. H. P. Brecht for technical assistance during the imaging experiments and M. P. Zamora for technical support in preparation of this manuscript.

## References and Notes

1. J. Perez-Juste, I. Pastoriza-Santos, L. M. Liz-Marzan, and P. Mulvaney, *Coordination Chemistry Reviews* 249, 1870 (2005).
2. P. M. Tiwari, K. Vig, V. A. Dennis, and S. R. Singh, *Nanomaterials* 1, 31 (2011).
3. A. Oraevsky, *Photoacoustic Imaging and Spectroscopy*, edited by L. Wang, Taylor and Francis Group, New York (2009).
4. B. C. Rostro-Kohanloo, L. R. Bickford, C. M. Payne, E. S. Day, L. J. Anderson, M. Zhong, S. Lee, K. M. Mayer, T. Zal, L. Adam, C. P. Dinney, R. A. Drezek, J. L. West, and J. H. Hafner, *Nanotechnology* 20, 434005 (2009).
5. C. K. Liao, S. W. Huang, C. W. Wei, and P. C. Li, *Journal of Biomedical Optics* 12, 064006 (2007).
6. X. Huang, I. H. El-Sayed, and M. A. El-Sayed, *Methods Mol. Biol.* 624, 343 (2010).
7. T. Niidome, M. Yamagata, Y. Okamoto, Y. Akiyama, H. Takahashi, T. Kawano, Y. Katayama, and Y. Niidome, *J. Control Release* 114, 343 (2006).
8. R. G. Rayavarapu, W. Petersen, L. Hartsuiker, P. Chin, H. Janssen, F. W. van Leeuwen, C. Otto, S. Manohar, and T. G. van Leeuwen, *Nanotechnology* 21, 145101 (2010).
9. C. S. Weisbecker, M. V. Merritt, and G. M. Whitesides, *Langmuir* 12, 3763 (1996).
10. M. J. Roberts, M. D. Bentley, and J. M. Harris, *Adv. Drug Del. Rev.* 54, 459 (2002).
11. H. P. Brecht, R. Su, M. Fronheiser, S. A. Ermilov, A. Conjusteau, and A. A. Oraevsky, *Journal of Biomedical Optics* 14, 064007 (2009).
12. R. Su, A. V. Liopo, H. P. Brecht, S. A. Ermilov, and A. A. Oraevsky, *Proceedings SPIE* (2011), Vol. 7899, p. 78994B.
13. M. Eghtedari, A. V. Liopo, J. A. Copland, A. A. Oraevsky, M. Motamedi, *Nano Letters* 9, 287 (2009).
14. B. Nikoobakht and M. A. El-Sayed, *Chemistry of Materials* 15, 1957 (2003).
15. T. K. Sau and C. J. Murphy, *Langmuir* 20, 6414 (2004).
16. A. V. Liopo, A. Conjusteau, M. Konopleva, M. Andreeff, and A. A. Oraevsky, *Proceedings SPIE* (2011), Vol. 7897, p. 789710.
17. O. V. Chumakova, A. V. Liopo, B. M. Evers, and R. O. Esenaliev, *Ultrasound Med. Biol.* 32, 751 (2006).
18. A. M. Alkilany and C. J. Murphy, *J. Nanopart. Res.* 12, 2313 (2010).
19. A. Kopwithaya, K. T. Yong, R. Hu, I. Roy, H. Ding, L. A. Vathy, E. J. Bergey, and P. N. Prasad, *Nanotechnology* 21, 315101 (2010).
20. H. Liao and J. H. Hafner, *Chemistry of Materials* 17, 4636 (2005).
21. W. P. Wueling, S. M. Gross, D. T. Miles, W. Royce, and R. W. Murray, *J. Am. Chem. Soc.* 120, 12696 (1998).
22. G. von Maltzahn, J. H. Park, A. Agrawal, N. K. Bandaru, S. K. Das, M. J. Sailor, and S. N. Bhatia, *Cancer Research* 69, 3892 (2009).
23. S. Motamedi, T. Shilagard, K. Edward, L. Koong, S. Qui, and G. Vargas, *Biomedical Optics Express* 2, 1194 (2011).
24. C. Lasagna-Reeves, D. Gonzalez-Romero, M. A. Barria, I. Olmedo, A. Clos, V. M. Sadagopa Ramanujam, A. Urayama, L. Vergara, M. J. Kogan, and C. Soto, *Biochem. Biophys. Res. Comm.* 393, 649 (2010).

Received: 31 January 2012. Accepted: 12 April 2012.